Leaky-Wave Antennas Using Artificial Dielectrics at Millimeter Wave Frequencies

I. J. BAHL, MEMBER, IEEE, AND PRAKASH BHARTIA, SENIOR MEMBER, IEEE

Abstract—**A novel approach for the design of leaky-wave antennas using artificial dielectrics at millimeter wave frequencies is discussed. The general radiation characteristics of leaky-wave structures of finite length are presented. The feasibility of frequency scanning and dielectric scanning (changing the direction of the beam by varying the relative permittivity of the electrically controlled liquid artificial dielectric medium) of a leaky-wave antenna using rodded artificial dielectric is investigated theoretically. Calculations shown that the beam angle changes from 20° to 50° off broadside when the frequency is changed from 31.1 to 35.4 GHz or the permittivity of the embedding medium of the artificial dielectric is changed from 1.6 to 2.04. Over a scan range of about 40° the beamwidth is almost constant. For large scan range, the beamwidth of a dielectric-scanned antenna (DSA) is about 15 percent less than the frequency-scanned antenna (FSA). The gain of a DSA is greater than the FSA and also has less variation over the scan range. The power efficiency is approximately the same for both the antenna types with worst case efficiency being about 85 percent.**

I. Introduction

SIGNIFICANT DEVELOPMENTS in millimeter wave technology have given rise to small, rugged, and high resolution radars. In addition, demands for military radars in missile, rocket, shell, and tank applications have generated a need for less complex, improved performance, low cost, electronically scannable antennas. Leaky-wave antennas have the potential of meeting these requirements, as evidenced by the literature on frequency scanning leaky-wave antennas using dielectric waveguides [1]–[7], dielectric rod antennas for millimeter wave integrated circuits [8], dielectric rod antennas integrated with an image line as a feed network for a frequency scanned array at millimeter wave frequencies [9], etc.

Leaky-wave antennas constitute a class of traveling wave antennas and are characterized by propagation of a leaky wave along an interface. These antennas are capable of providing very narrow beams, can be flush mounted (for example, with the missile body), are easily matched at the input and output ports and possess electronic (frequency and dielectric) scanning characteristics.

The leaky-wave antenna using inverted strip dielectric guide has the disadvantage of low leakage energy. It has been pointed out in [10] that periodic loading of a basically slow wave structure produces a complex wave which continuously radiates power in space but with the bulk of the guided energy being bound. This bound energy for small length antennas is generally larger than the radiated power. Thus the antenna radiates in the endfire direction [5].

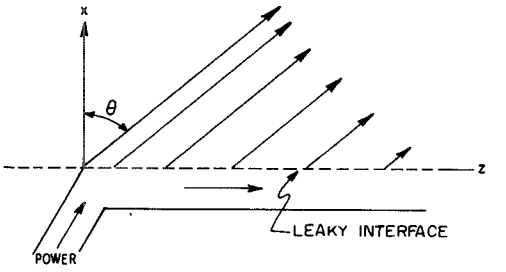

Fig. 1. Radiation from a leaky interface.

In the present paper, the design considerations for leaky-wave antennas are reviewed. Potential structures for millimeter wave leaky-wave antennas are described. Radiation characteristics of an artificial dielectric structure as a millimeter wave leaky-wave antenna are investigated theoretically. Electronic scanning using variable frequency as well as variable dielectric constant employing a rodded artificial dielectric structure is explored.

II. Review of Leaky-Wave Antennas

A leaky-wave antenna may be simply defined as the guiding structure which conveys guided waves accompanied by radiation into space as shown in Fig. 1. The radiated waves are excited by the guided waves traveling along the uniform or periodically loaded guiding structure with complex propagation constant γ. Although the theoretical basis for leaky waves has long been discussed [11]–[16], this section reviews the leaky-wave antennas from the design point of view.

Expressions for the radiation characteristics of such structures are given in Table I. The angle θ is measured from the normal to the antenna interface. $\gamma=\beta+j\alpha$, where β and α are the real and imaginary parts of the propagation constant normalized with respect to free space propagation constant $k_0=2\pi/\lambda_0$. The antenna aperture has dimensions of length L and width W, and α_c is the normalized attenuation constant due to ohmic and dielectric losses in the structure.

The Kirchhoff–Huygens method has been used in the derivations of the above expressions and the antenna is excited from one end. It is assumed that the structure is

Manuscript received December 5, 1979; revised July 8, 1980. This work was supported the Natural Sciences and Engineering Council of Canada under Grant A-0001.

I. J. Bahl is with the Department of Electrical Engineering, University of Ottawa, Ottawa, Canada K1N 6N5.

P. Bhartia is with the Defence Electronics Division, Defence Research Establishment, Ottawa, Canada K1A 0Z4.

0018-9480/80/1100-1205$00.75 ©1980 IEEE

TABLE I
DESIGN EXPRESSIONS FOR A LEAKY-WAVE ANTENNA (THE EXPRESSIONS ARE VALID FOR AN UNIFORM PLANAR STRUCTURE EXCITED AT ONE END AND RADIATING INTO UPPER HEMISPHERE)

Expressions for Radiation Characteristics	Reference
Radiation Pattern in H-plane, $R(\theta)$	
$R(\theta) = \lvert\cos\theta \cdot \sin[d(\sin\theta-\gamma)]/[d(\sin\theta-\gamma)]\rvert^2$ where $d = k_o L/2$	[15], [18]
Beam Direction, θ_m	
$\theta_m = \sin^{-1}\left[\frac{1+\beta^2+\alpha^2 - \{(1+\beta^2+\alpha^2)^2-4\beta^2\}^{\frac{1}{2}}}{2\beta}\right]$	[17]
$\theta_m = \sin^{-1}(\beta)$ for $\alpha \ll \beta$	
Beamwidth, BW(radians)	
$BW = \sin^{-1}\{\beta + (\lvert A\rvert+0.165)/d\} - \sin^{-1}\{\beta - (\lvert A\rvert+0.165)/d\}$	[18]
where	
$\lvert A\rvert = 0.866\left\{-\left[\frac{\sinh^2(\alpha d)}{(\alpha d)^2} - 2\right] + \left[\left\{\frac{\sinh^2(\alpha d)}{(\alpha d)^2} - 2\right\}^2 + 2.667\sinh^2(\alpha d)\right]^{\frac{1}{2}}\right\}^{\frac{1}{2}}$	
Gain, G	
$G = \cos\theta_m[4\pi WL/\lambda_0^2][\tanh(\alpha d)/(\alpha d)]$	[17]
Side-lobe Level, SL	
$SL(-dB) = 10\log\left[\frac{\{(3\pi/2)^2+(\alpha d)^2\}\{(1-\beta^2)\tanh^2(\alpha d)/(\alpha d)^2\}}{1-(\beta-1.5\pi/d)^2}\right]$	[17]
Efficiency, η	
$\eta\ \% = 100(1-\alpha_c/\alpha)[1-e^{-4\alpha d}]$	[17]

uniform, i.e., the propagation constant does not vary along its length. It is also assumed that either the remaining power at the far end of the antenna is negligible because of leakage, ohmic, and dielectric losses, or that the antenna is terminated in a resistive matching arrangement. These expressions for the radiation characteristics will be used for designing leaky-wave antennas at millimeter wave frequencies.

III. LEAKY-WAVE STRUCTURES

Structures for leaky-wave antennas at millimeter wave frequencies can be divided into two categories: perturbed waveguide type (Fig. 2(a)) and open guiding type (Fig. 2(b)). Slotted waveguide [10], [20], thin wall waveguide [21], inductive grid waveguide [22], and grounded artificial dielectric slab [16], [18], [19], [23]–[25] structures have been studied at microwave frequencies whereas the inverted strip dielectric guide [1]–[5] and dielectric guide with conducting perturbations [6], [7] have been studied at millimeter wave frequencies. In the present paper, artificial dielectric filled waveguide and the grounded artificial dielectric slab will be discussed. The artificial dielectric used is shown in Fig. 3. It consists of a two-dimensional array of conducting wires embedded in a lossless dielectric medium. The dielectric medium may be a dielectric material or a liquid artificial dielectric [26]. When an electromagnetic wave propagates in a direction perpendicular to the direction of the wires with the electric field

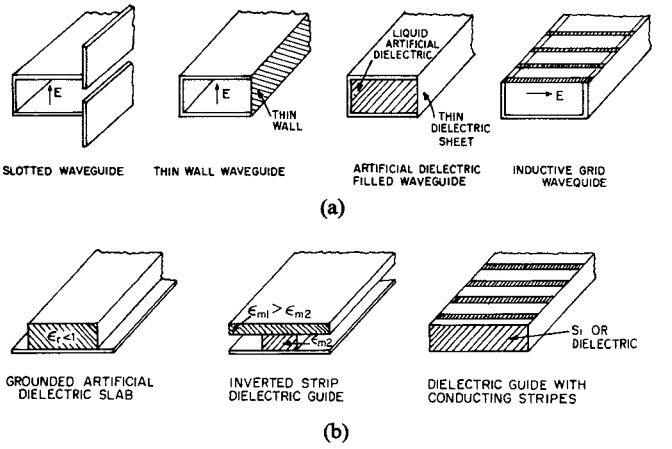

Fig. 2. Various structures for leaky-wave antennas at millimeter wave frequencies. (a) Perturbed waveguide. (b) Open guiding.

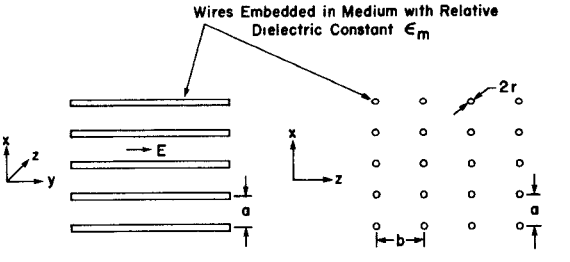

Fig. 3. Artificial dielectric structure consisting of two-dimensional array of wires embedded in medium of dielectric constant ϵ_m.

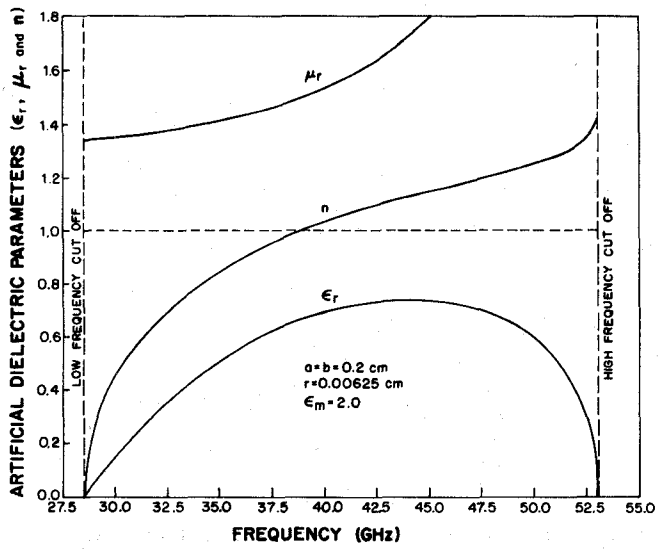

Fig. 4. Variation of parameters of artificial dielectric with frequency.

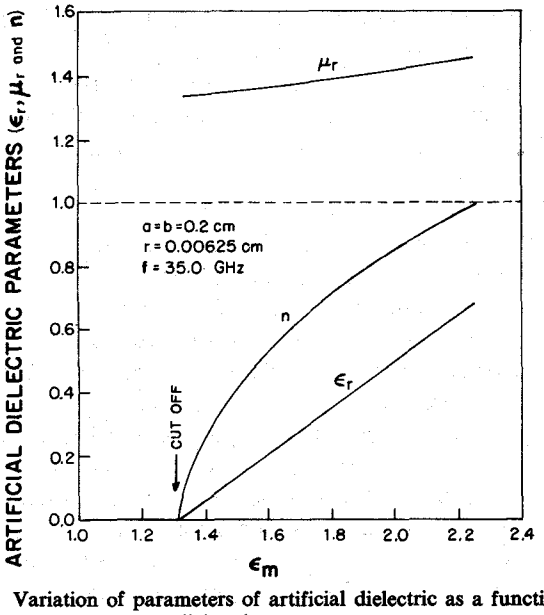

Fig. 5. Variation of parameters of artificial dielectric as a function of dielectric constant.

component in the direction of the wires (as in the TE mode), the structure has effective relative permittivity ϵ_r less than unity. Such a medium is called a phase advance artificial dielectric [27]–[29] and supports fast leaky waves [18].

The effective relative permittivity, the effective relative permeability μ_r and the index of refraction n for this structure are calculated using the analysis given in the appendix. Results are shown in Fig. 4 as a function of frequency and in Fig. 5 as a function of dielectric constant. These structures have low frequency as well as high frequency cutoffs. In the case of Fig. 4, the artificial dielectric (AD) parameters are plotted between the two cut off frequencies whereas in Fig. 5, the AD parameters as a function of ϵ_m are shown only for $n \leqslant 1$, where ϵ_m is the relative permittivity of the embedding medium. Values of dielectric constant for few controllable liquid artificial dielectric medium are given in [26]. In most cases $\epsilon_m \simeq 2$.

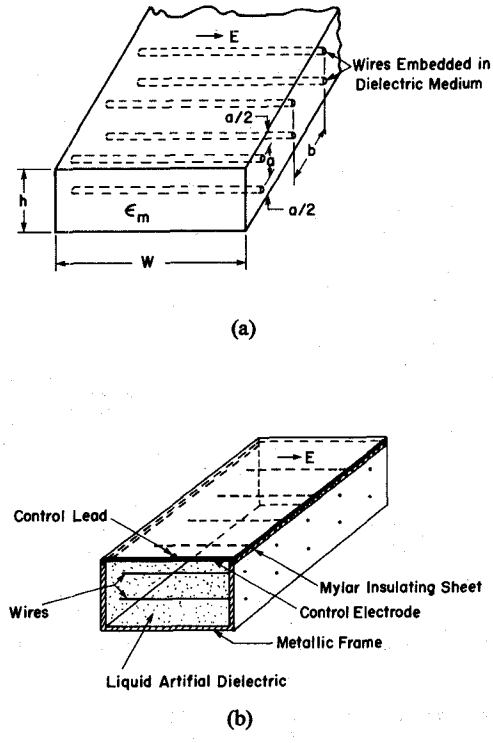

Fig. 6. Artificial dielectric slab. (a) Dielectric material as a embedding medium. (b) Liquid artificial dielectric as a embedding medium.

A. Propagation Constant of the Structure

The radiation characteristics of leaky-wave antennas described above are determined by the propagation constant γ which can be obtained by solving Maxwell's equations with the associated boundary conditions, or by using a transverse resonance technique or by a variational formulation. For some structures, usually the open type, it is possible to formulate the boundary value problem, obtain the dispersion relation and solve for γ.

The geometry of the configuration to be analyzed is shown in Fig. 6. The AD slab shown in Fig. 6(a) uses solid dielectric material as a embedding medium while in Fig. 6(b) the embedding medium is a liquid artificial dielectric. The thickness of the AD slab is h. The structure is assumed to be infinite along the y-direction. Only TE modes are considered because the refractive index of the AD is less than unity for these modes. A simple expression for the normalized propagation constant γ for TE_{m0} modes (the suffix m denotes half-sine variation of field in the AD slab along the x-direction, while the second suffix 0 signifies that there is no variation of field along the y-direction as assumed earlier) is obtained in the same way as it was obtained for the dominant TE_{10} mode [18]. This expression is given by

$$\gamma = \left[\epsilon_r \mu_r - \left(\frac{m\pi}{k_0 h} \right)^2 \cdot \left\{ 1 - \frac{1}{1 + (-1)^m \mu_r \{ k_0^2 h^2 (\epsilon_r \mu_r - 1) - (m\pi)^2 \}^{1/2}} \right\}^2 \right]^{1/2} \quad (1)$$

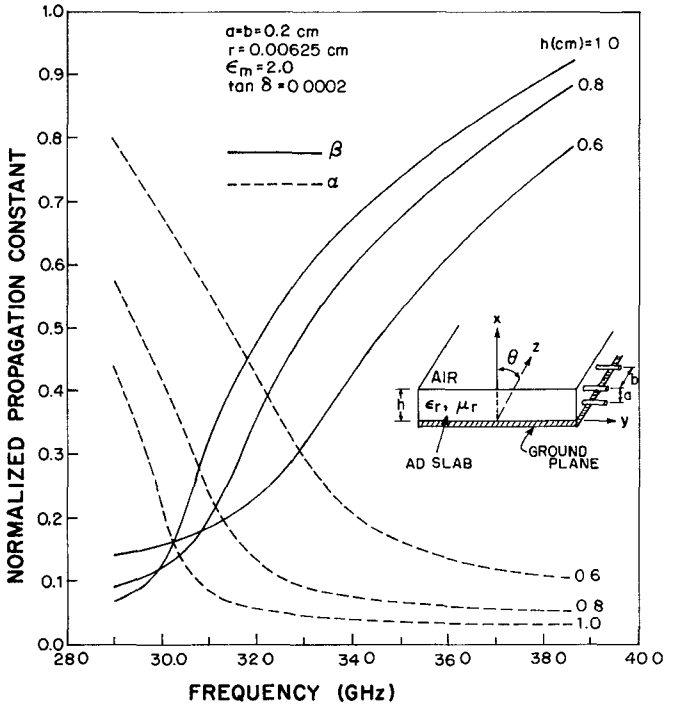

Fig. 7. Normalized propagation constant (real and imaginary parts) as a function of frequency.

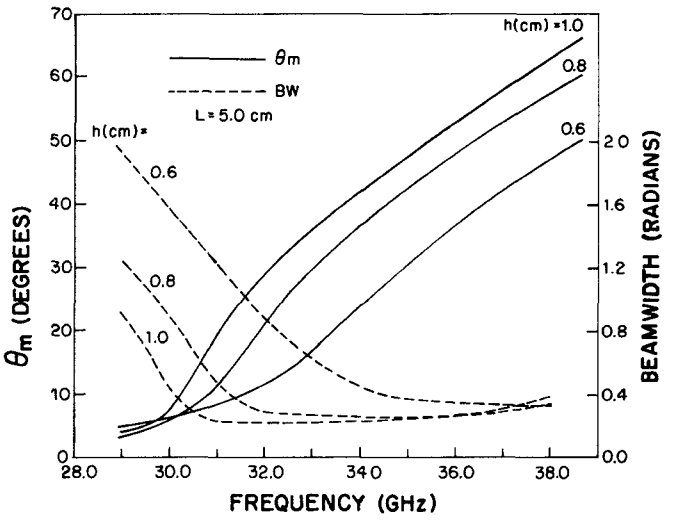

Fig. 8. Variation of beam direction and beamwidth with frequency of a frequency-scanned antenna.

and may be used to calculate the propagation constant for any mode. In deriving this expression, the *AD* slab is assumed lossless. However, since the loss due to radiation is much larger than the ohmic and dielectric losses, the latter two losses will be considered separately.

Values of normalized propagation constant $\gamma=(\beta+j\alpha)$ calculated at various frequencies by using (1) for $a=b=0.2$ cm, $r=0.00625$ cm, $\epsilon_m=2.0$, and for various values of h are shown in Fig. 7. The mode assumed here is the dominant TE_{10} mode. The attenuation constant α decreases with the increase in the value of h and the phase constant β increases with increase in the value of h at higher frequencies only (above 30 GHz).

IV. Electronic Scanning

Most of the leaky-wave antennas are capable of changing the direction of the radiated beam with change of frequency. In these antennas, scanning is achieved as a result of the frequency dependence of the complex propagation constant. In the present structure the complex propagation constant can be changed by changing the frequency or by changing the dielectric constant of the embedding medium as in the case of electrically controlled liquid artificial dielectrics [26]. In general, the direction of the radiated beam is given by $\theta_m=\sin^{-1}(\beta)$. In the case of thin-wall leaky-wave antennas and liquid artificial dielectric filled waveguide antennas, θ_m is given by

$$\theta_m=\sin^{-1}\left[\epsilon_m-\left(\frac{\lambda_0}{2a}\right)^2\right]^{1/2} \tag{2}$$

where a is the broad dimension of the waveguide. Both the frequency scanning and the dielectric scanning (i.e., changing the permittivity of the liquid artificial dielectric medium by varying the amplitude of the applied low frequency voltage) techniques will now be considered. Because scan angle varies with frequency, the more dispersive the structure the faster the scanning.

A. Frequency Scanning

If the *AD* structure is to be used as a frequency scanned antenna the dielectric constant of the embedding medium should be greater than unity (Appendix, Fig. 15). The parameters of the *AD* change faster with frequency when the dielectric constant of the embedding medium is increased. Hence the frequency range over which the refractive index varies from 0 to 1 gets reduced and the scan rate (change in θ_m per unit frequency) is increased.

The variations of beam position and beamwidth with frequency for various values of h are shown in Fig. 8. For $h=1.0$ cm, the scan rate is almost constant from 20° to 65°. It is noted that the beam angle changes from 10° to 65° off broadside when the frequency is varied from 30.3 to 38.8 GHz. For the parameters considered, the value of scan rate is 6°/GHz. As pointed out earlier, higher scan rates may be obtained by increasing the dielectric constant value of the embedding medium. It is found that the present structure (*AD*) is much more dispersive, i.e., $\Delta\theta_m/\Delta f$ is larger than the insular guide studied for frequency scanned array [9], silicon waveguide with metallic stripe perturbations used for frequency scanned antenna [6] and inverted strip dielectric waveguide [2], [5] when the same dielectric material is used.

The beamwidth as shown in Fig. 8 does not vary monotonically. The beamwidth decreases with the increase in the value of h. This figure shows that the beamwidth of an *AD* antenna increases rapidly when the frequency approaches the low frequency cutoff. In the present case for $h=1.0$ cm, the beamwidth is almost constant over the frequency range of 30.35 to 36.0 GHz. The gain for this antenna is shown is Fig. 9 and is

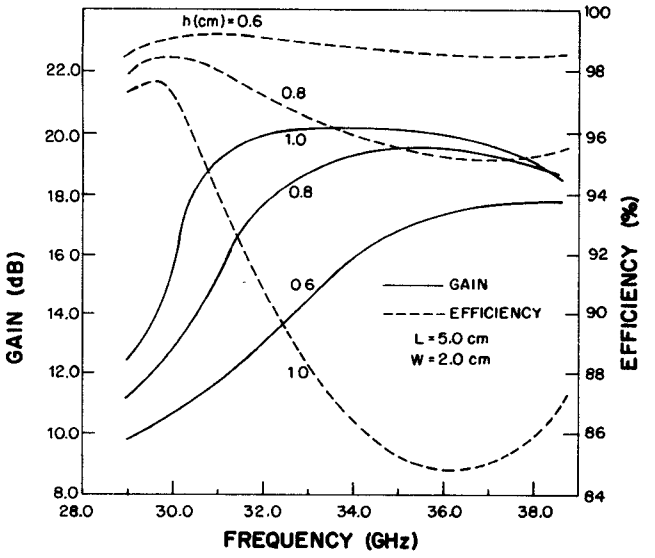

Fig. 9. Gain and efficiency of a frequency-scanned antenna as a function of frequency.

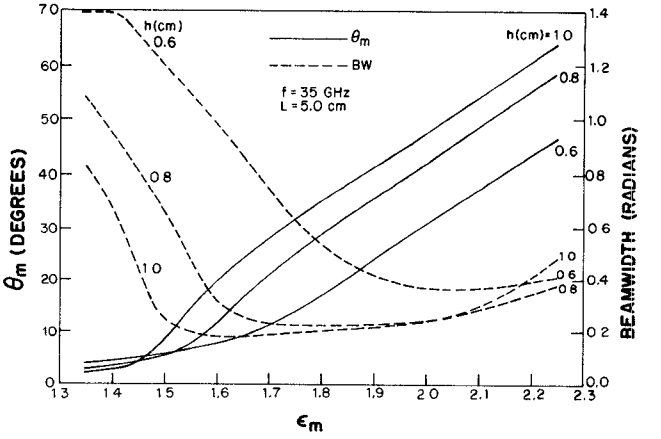

Fig. 10. Variation of beam direction and beamwidth with dielectric constant of a dielectric-scanned antenna.

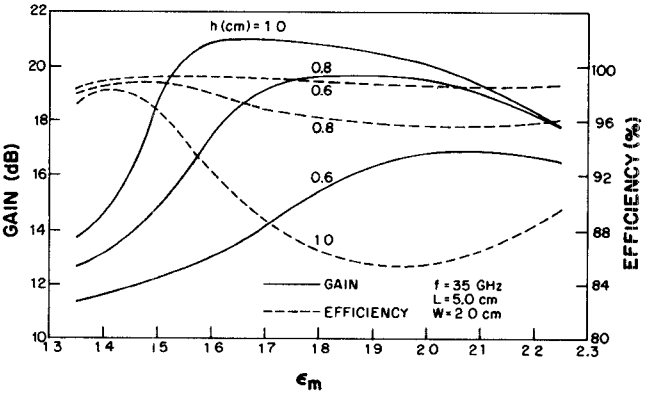

Fig. 11. Gain and efficiency of a dielectric-scanned antenna as a function of dielectric constant.

constant for this frequency range. Further, the variation of efficiency of this frequency-scanned antenna is also shown in Fig. 9. Maximum efficiency is available when the height of the *AD* slab is small. This is because of the fact that for smaller heights the attenuation due to radiation is much more than the attenuation due to ohmic losses. In the worst case, the efficiency obtained for $h=1.0$ cm in the frequency range, 30.35 to 36 GHz is about 85 percent.

B. Dielectric Scanning

For dielectric scanned leaky-wave antennas, fast scanning can be obtained by using liquid artificial dielectrics of high relative permittivity. The variations of beam position and the beamwidth as a function of dielectric constant are shown in Fig. 10. In this case also the scan rate is almost constant from 20° to 65°. The scan rate $(\Delta\theta_m/\Delta\epsilon_m)$ is $70°/(\Delta\epsilon_m=1)$. The beamwidth is nearly constant over the scan range of 8° to 50°. The gain and the efficiency are plotted in Fig. 11. For $h=1.0$ cm, the gain is almost constant over the scan range. As in the case of frequency scanning, the efficiency is higher for smaller heights of the *AD* slab. The worst case efficiency for $h=1.0$ cm is about 85 percent.

C. Comparison of Frequency and Dielectric Scanned Antennas

Angle scanning characteristics of frequency-scanned and dielectric-scanned antennas are compared in Table II. For this comparison, $h=1.0$ cm and the same angle scan ranges are selected to obtain minimum variation in beamwidth and gain.

From Table II it is noted that for small scan ranges (20°–50°), the frequency scanned antenna (FSA) has less variation in the beamwidth as compared to the dielectric-scanned antenna (DSA). The gain of a dielectric-scanned antenna is greater by about 0.8 dB over the frequency-scanned antenna. Efficiency is more or less the same for both the types in the case of small scan ranges as well as for large scan ranges. For large scan range (10°–55°), the maximum and minimum gains of DSA are 21.0 dB and 19.2 dB, respectively, compared to 20.2 dB and 17.0 dB for the FSA. It is thus noted that the FSA has more variation in the gain of the antenna in comparison to the DSA. Variation in the beamwidth is almost the same for both techniques, although the DSA has about 15 percent less beamwidth than the FSA. Thus it may be concluded that for large scan ranges, a dielectric-scanned antenna has better scanning characteristics than a frequency-scanned antenna.

APPENDIX

DESIGN OF AN ARTIFICIAL DIELECTRIC MEDIUM

An artificial dielectric medium using a two-dimensional array of conducting wires is shown in Fig. 3. The wires are embedded in a dielectric medium whose loss tangent is very small. For finite conductivity of the wires, the complex propagation constant is given by [27]–[29]

$$\cosh(\gamma_r b)=\cos\left(\sqrt{\epsilon_m}\,B\right)+j\frac{Z_0}{2Z_t\sqrt{\epsilon_m}}\sin\left(\sqrt{\epsilon_m}\,B\right) \quad (3)$$

TABLE II
COMPARISON BETWEEN FREQUENCY-SCANNED AND DIELECTRIC-SCANNED ANTENNAS AT MILLIMETER WAVE FREQUENCIES ($L=5.0$ cm and $W=2.0$ cm)

Characteristics	Angle scan range (Degrees)			
	20 - 50		10 - 55	
	Frequency Scanning	Dielectric Scanning	Frequency Scanning	Dielectric Scanning
Frequency range (GHz)	31.1-35.4	35.0	30.0-36.4	35.0
Dielectric constant range	2.0	1.6-2.04	2.0	1.51-2.115
Beamwidth(radians) Min.	0.21	0.18	0.21	0.18
Max.	0.24	0.26	0.34	0.30
Gain (dB) Min.	19.2	19.9	17.0	19.2
Max.	20.2	21.0	20.2	21.0
Efficiency(%) Min.	85.0	85.3	84.8	85.3
Max.	93.5	92.3	96.5	96.0

where

B $2\pi b/\lambda_0$;
b spacing between the wires in the direction of propagation;
λ_0 free space wavelength;
$\gamma_r=\alpha_r+j\beta_r$ the complex propagation constant in the rodded artificial dielectric;
ϵ_m the relative dielectric constant of the embedding medium;
$Z_0=120\pi\ \Omega$ impedance of free space;
Z_t the shunt impedance of the wire grid.

The shunt impedance Z_t of a grid of lossy wires is composed of two parts [30]: the internal impedances of the wires $Z_i=(R_i+jX_i)$ and the reactance (X_g) of a parallel wire grid in a plane normal to the direction of propagation [31]. Thus

$$Z_t=Z_i+jX_g=R_i+j(X_i+X_g). \tag{4}$$

The shunt reactance of a grid for $r\ll a$ (where r is the radius of the wires and a is the spacing between the wires of a grid), and the resistive components of the internal impedance of a single wire are given by

$$X_g\simeq\frac{Z_0 a}{\lambda_0}\ln\left(\frac{a}{2\pi r}\right) \tag{5}$$

$$R_i=\frac{R_s}{\sqrt{2}\,\pi r}\left[\frac{J_{0r}\cdot J'_{0i}-J_{0i}\cdot J'_{0r}}{(J'_{0r})^2+(J'_{0i})^2}\right],\quad \Omega/\text{unit length} \tag{6}$$

$$X_i=\frac{R_s}{\sqrt{2}\,\pi r}\left[\frac{J_{0r}\cdot J'_{0r}+J_{0i}\cdot J'_{0i}}{(J'_{0r})^2+(J'_{0i})^2}\right],\quad \Omega/\text{unit length} \tag{7}$$

where R_s is the resistivity of the wires ($\sqrt{\pi\mu_0 f/\sigma}$), J_{0r} and J_{0i} are the real and imaginary parts of the Bessel function $J_0(x)$ of order zero and complex argument $x=(1-j)r/\delta$). The prime sign stands for the derivative, δ is the penetration depth ($1/\sqrt{\pi\mu_0 f\sigma}$), μ_0 is free space permeability, and σ is the conductivity of the wires. For copper wires

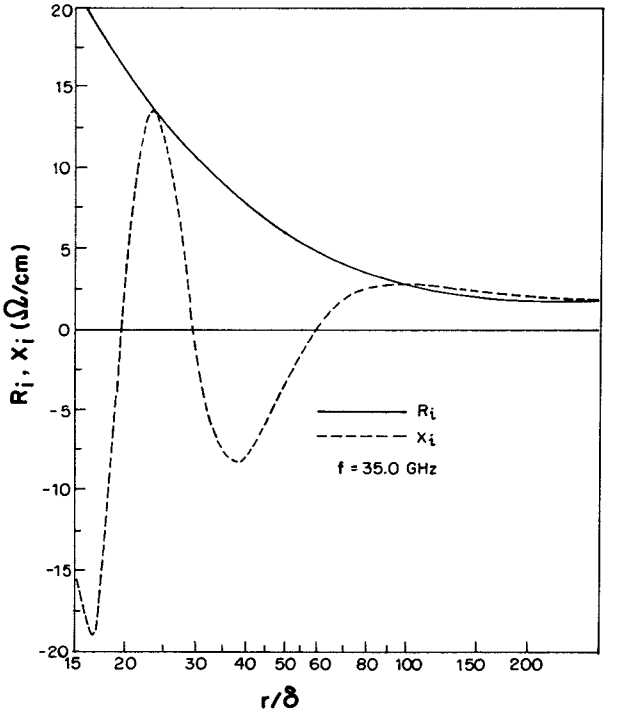

Fig. 12. Real and imaginary parts of internal impedance of a copper wire as a function of its normalized radius with respect to skin depth.

the surface resistivity and the penetration depth may be written as

$$R_s=2.6\times10^{-7}\sqrt{f}\ \Omega \tag{8}$$

$$\delta=6.5/\sqrt{f}\ \text{cm}. \tag{9}$$

Variations of the real and imaginary parts of the internal impedance as a function of the r/δ ratio for $f=35$ GHz are shown in Fig. 12. The resistive part decreases monotonically with r/δ and the reactive part is oscillatory in nature for small values of r/δ and decreases monotonically for large values of r/δ. For $r/\delta>100$, R_i and X_i have nearly the same values. R_i and X_i versus frequency for various values of the radius of the copper wire are shown

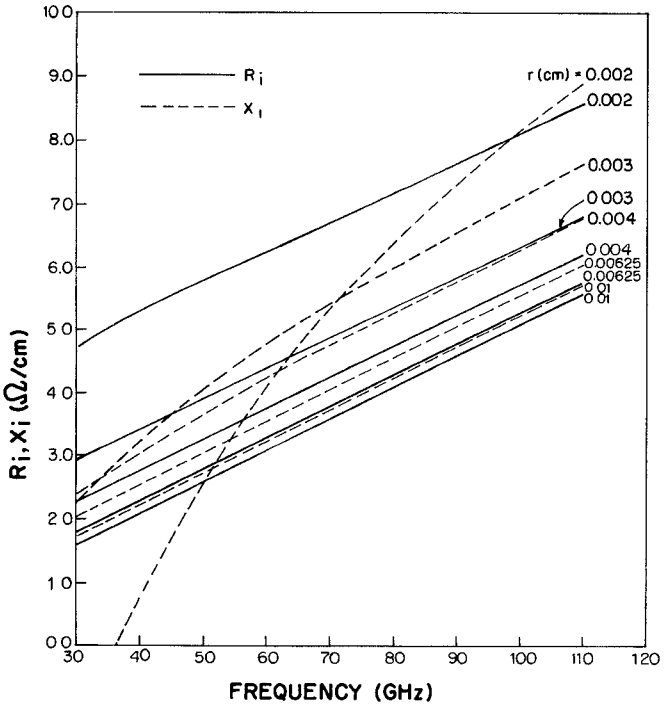

Fig. 13. Real and imaginary parts of internal impedance of a copper wire as a function of frequency for various values of its radius.

in Fig. 13. For $r \geq 0.004$ cm, R_i and X_i increase linearly with frequency. For $r=0.00625$, the expressions for the internal resistance and reactance can be written as

$$R_i = 1.8 + 0.05(f-30)\ \Omega/\text{cm} \tag{10}$$

$$X_i = 2.02 + 0.051(f-30)\ \Omega/\text{cm} \tag{11}$$

where $f(\text{GHz}) \geq 25$. These expressions have an accuracy better than 0.5 percent.

For moderate attenuation in the structure, i.e., $\alpha_r \ll \beta_r$, (3) may be written as

$$\cos(nB) \simeq \cos\left(\sqrt{\epsilon_m}\, B\right) + \frac{(X_i+X_g)Z_0}{2\left\{R_i^2+(X_i+X_g)^2\right\}\sqrt{\epsilon_m}} \sin\left(\sqrt{\epsilon_m}\, B\right) \tag{12}$$

$$\alpha_r \simeq \frac{R_i Z_0}{2b\left\{R_i^2+(X_i+X_g)^2\right\}\sqrt{\epsilon_m}} \sin\left(\sqrt{\epsilon_m}\, B\right)/\sin(nB), \quad \text{nepers/unit length} \tag{13}$$

where

$$n = \frac{\lambda_0}{2\pi}\beta_r$$

is the effective index of refraction of the artificial dielectric medium. If the loss in the embedding medium due to its finite conductivity is also considered then the total attenuation constant becomes

$$\alpha_s = \alpha_r + \alpha_d \tag{14}$$

where

$$\alpha_d = \pi\sqrt{\epsilon_m}\tan\delta/\lambda_0, \quad \text{nepers/unit length} \tag{15}$$

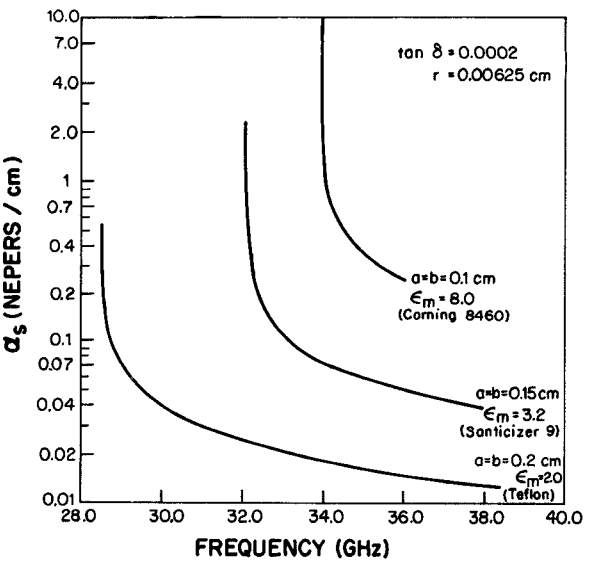

Fig. 14. Attenuation constant due to ohmic and dielectric losses in an infinite artificial dielectric structure.

and $\tan\delta$ is the loss tangent of the embedding dielectric medium.

Variations of the total loss, α_s Np/cm in the AD structure as a function of frequency for various values of the spacing between the wires is shown in Fig. 14. As the spacing between the wires increases the structure loss decreases. The loss decreases monotonically with the frequency.

The effective relative permittivity and the effective relative permeability of the AD medium have been obtained [32] and can be derived as follows. The characteristic impedance Z_r of the rodded medium is given by [28]

$$Z_r = \frac{Z_0}{\sqrt{\epsilon_m}}\tan\left(\sqrt{\epsilon_m}\, B/2\right)/\tan(nB/2). \tag{16}$$

For a plane wave, the characteristic impedance of the medium with relative permittivity ϵ_r and relative permeability μ_r can be written as

$$Z_r = Z_0\sqrt{\frac{\mu_r}{\epsilon_r}}\ . \tag{17}$$

From (16) and (17) and $n=\sqrt{\epsilon_r\mu_r}$

$$\epsilon_r = n\sqrt{\epsilon_m}\tan(nB/2)/\tan\left(\sqrt{\epsilon_m}\, B/2\right) \tag{18}$$

$$\mu_r = \frac{n}{\sqrt{\epsilon_m}}\tan\left(\sqrt{\epsilon_m}\, B/2\right)/\tan(nB/2). \tag{19}$$

The low frequency cutoff of the structure is obtained by solving

$$\cos\left(\sqrt{\epsilon_m}\, B\right) + \frac{(X_i+X_g)Z_0}{2\left\{R_i^2+(X_i+X_g)^2\right\}\sqrt{\epsilon_m}} \sin\left(\sqrt{\epsilon_m}\, B\right) = \pm 1 \tag{20}$$

whereas the high frequency cutoff is given by

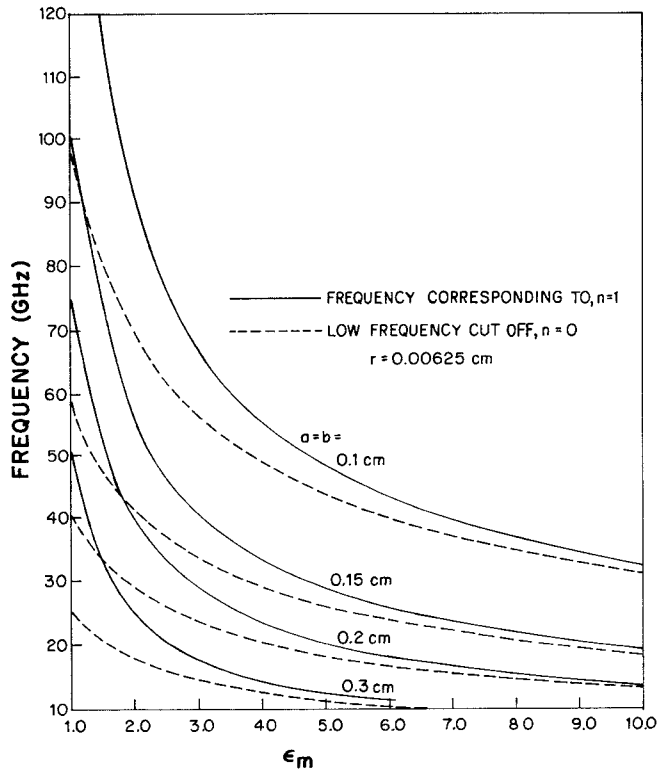

Fig. 15. Variations of low frequency cutoff and the frequency corresponding to $n=1$ as a function of dielectric constant of the embedding medium for various AD structures.

$$f_{hc}=\frac{15}{b\sqrt{\epsilon_m}}\text{(GHz)} \tag{21}$$

where b is in centimeters. Variations of frequencies corresponding to $n=1$ and $n=0$ as a function of ϵ_m for various values of wires spacing are plotted in Fig. 15.

Acknowledgment

The authors wish to thank Prof. W. J. R. Hoefer for helpful suggestions.

References

[1] T. Itoh, "Leaky-wave antenna and band-reject filter for millimeter-wave integrated circuits," in *1977 IEEE MTT-S Int. Microwave Symp. Dig.*, (San Diego, CA), June 21–23, 1977, pp. 538–541.

[2] T. Itoh and A. S. Hebert, "Simulation study of electronically scannable antennas and tunable filters integrated in a quasi-planar dielectric waveguide," in *1978 IEEE MTT-S Int. Microwave Symp. Dig.*, (Ottawa, Canada), June 27–29, 1978, pp. 30–32.

[3] A. A. Oliner, S. T. Peng, and J. P. Hsu, "New propagation effects for the inverted strip dielectric waveguide for millimeter waves," in *1978 IEEE MTT-S Int. Microwave Symp. Dig.*, (Ottawa, Canada), June 27–29, 1978. pp. 408–410.

[4] T. Itoh, "Application of gratings in a dielectric waveguide for leaky-wave antennas and band-reject filters," *IEEE Trans. Microwave Theory Tech.*, vol. MTT-25, pp. 1134–1138, Dec. 1977.

[5] T. Itoh and A. S. Hebert, "Simulation study of electronically scannable antennas and tunable filters integrated in a quasiplanar dielectric waveguide," *IEEE Trans. Microwave Theory Tech.*, vol. MTT-26, pp. 987–991, Dec. 1978.

[6] K. L. Klohn *et al.*, "Silicon waveguide frequency scanning linear array antenna," *IEEE Trans. Microwave Theory Tech.*, vol. MTT-26, pp. 764–773, Oct. 1978.

[7] K. Solbach, "*E*-band leaky wave antenna using dielectric image line with etched radiating elements," in *1979 IEEE MTT-S Int. Microwave Symp. Dig.*, (Orlando, FL), 1979, pp. 214–216.

[8] Y. Shiau, "Dielectric rod antennas for millimeter-wave integrated circuits," *IEEE Trans. Microwave Theory Tech.*, vol. MTT-24, pp. 869–872, Nov. 1976.

[9] N. Williams, A. Rudge, and S. Gibbs, "Millimeter-wave insular-guide frequency scanned array," in *1977 IEEE MTT-S Int. Symp. Dig.*, (San Diego, CA), June 21–23, 1977, pp. 542–544.

[10] R. E. Collins and F. J. Zucker, *Antenna Theory, Part II.* New York: McGraw Hill, 1969, p. 185.

[11] N. Marcuvitz, "On field representation in terms of leaky modes or eigenmodes," *IRE Trans. Antennas Propagat.*, vol. AP-4, pp. 192–194, July 1956.

[12] T. Tamir and A. A. Oliner, "The influence of complex waves on the radiation field of a slot excited plasma layer," *IRE Trans. Antennas Propagat.*, vol. AP-10, pp. 55–65, Jan. 1962.

[13] E. S. Cassedy and M. Cohn, "On the existence of leaky waves due to a line source above a grounding dielectric slab," *IRE Trans. Microwave Theory Tech.*, vol. MTT-9, pp. 234–247, May 1961.

[14] T. Tamir and A. A. Oliner, "Guided complex waves, Part I, Fields at an interface," *Proc. Inst. Elec. Eng.*, vol. 110, pp. 310–324, Feb., 1963.

[15] R. E. Collins and F. J. Zucker, *Antenna Theory, Part II.* New York: McGraw-Hill, 1969, ch. 20.

[16] K. C. Gupta, "Narrow beam antenna using an artificial dielectric medium with permittivity less than unity," *Electron. Lett.*, vol. 7, no. 1, p. 16, Jan. 1971.

[17] I. J. Bahl and K. C. Gupta, "Design considerations for leaky-wave antennas," *Proc. Inst. Elec. Eng.*, vol. 123, pp. 1302–1306, Dec. 1976.

[18] I. J. Bahl and K. C. Gupta, "A leaky-wave antenna using an artificial dielectric medium," *IEEE Trans. Antennas Propagat.*, vol. AP-22, pp. 119–122, Jan. 1974.

[19] K. C. Gupta, I. J. Bahl, and R. Garg, "Characteristics of leaky wave antennas—a review," *Summaries of Papers, Int. Symp. Antennas and Propagation*, (Japan), pp. 531–534, 1978.

[20] C. H. Walter, *Travelling Wave Antennas.* New York: McGraw-Hill, 1965, ch. 4.

[21] Ramesh Garg, K. C. Gupta, and R. Saran, "A thin wall leaky-waveguide antenna," *IEEE Trans. Antennas Propagat.*, vol. AP-23, pp. 107–112, Jan. 1975.

[22] R. C. Honey, "A flush-mounted leaky-wave antenna with predictable patterns," *IRE Trans. Antennas Propagat.*, vol. AP-7, pp. 320–329, Oct. 1959.

[23] I. J. Bahl and K. C. Gupta, "Frequency scanning by leaky-wave antennas using artificial dielectrics," *IEEE Trans. Antennas Propagat.*, vol. AP-23, pp. 584–589, July 1975.

[24] I. J. Bahl and K. C. Gupta, "Radiation from a dielectric-artificial dielectric slab," *IEEE Trans. Antennas Propagat.*, vol. AP-24, pp. 73–76, Jan. 1976.

[25] I. J. Bahl and K. C. Gupta, "A multiple beam antenna using grounded artificial dielectric slab," *J. Inst. Electron. Telecom. Engrs.* (India), vol. 22, pp. 778–780, Dec. 1976.

[26] H. T. Buscher, "Electrically controlled liquid artificial dielectric media," *IEEE Trans. Microwave Theory Tech.*, vol. MTT-27, pp. 540–545, May 1979.

[27] J. Brown, "Artificial dielectrics having refractive indices less than unity," Proc. Inst. Elec. Eng. vol. 100 IV, pp 51–62, Jan., 1953.

[28] W. Rotman, "Plasma simulation by artificial dielectrics and parallel plate media," *IRE Trans. Antennas Propagat.*, vol. AP-10, pp. 82–95, Jan. 1962.

[29] J. B. Birks and J. H. Schulman, *Progress in Dielectrics.* London, England: Heywood, 1960, pp. 213–214.

[30] E. A. Lewis and J. P. Casey, "Reflection and transmission by resistive gratings," *J. Appl. Phys.*, vol. 23, p. 605, June 1952.

[31] S. Ramo and J. R. Whinnery, *Fields and Waves in Modern Radio.* New York: Wiley, 1953, pp. 242–248.

[32] I. J. Bahl, "Leaky-wave antennas using artificial dielectrics," Ph.D. thesis, Dep. Elec. Eng., Indian Inst. Tech., Kanpur, India, May 1974.